APPENDIX G:
REFLECTION FROM A PLANE PLACED NEAR THE FOCUS AT ARBITRARY ANGLE

In this appendix, the voltage received by the ultrasound source when a reflecting plane is placed in the focal region will be derived. The plane will be later used to approximate the skull interface when imaging the developing fetal brain. The velocity potential field in the focal region is approximated by a three-dimensional Gaussian. The coordinate system for the problem is shown in Figure G.1. In this figure, $\vec{n}_f$ is the outward normal for the plane that intersects the z-axis at a distance of z_o from the focus (positive for z_p>0) with n_{fx}, n_{fy}, n_{fz} given by

$$\begin{aligned} n_{fx}\hat{x} &= \sin(\theta_f)\cos(\phi_f)\hat{x} \\ n_{fy}\hat{y} &= \sin(\theta_f)\sin(\phi_f)\hat{y} \\ n_{fz}\hat{z} &= \cos(\theta_f)(-\hat{z}). \end{aligned} \tag{G.1}$$

Hence, the equation describing the plane is given by

$$x\cdot\sin(\theta_f)\cos(\phi_f)+y\cdot\sin(\theta_f)\sin(\phi_f)+(z_p-z)\cdot\cos(\theta_f)=0. \tag{G.2}$$

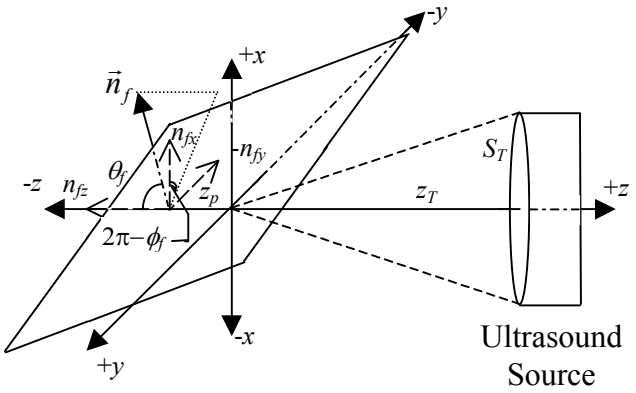

Figure G.1: Coordinate system for reflection from plane placed in the focal region.

The goal is to solve for the reflected longitudinal waves in the region of the ultrasound source. Shear waves were not included in the initial developments in order to simplify the analysis. The impact of neglecting shear waves is beyond the scope of the current work, but in general, the influence of shear waves on the reflected longitudinal waves is small when the incident angle of the wave with respect to the plane normal is small [*Mayer*, 1964]. Hence, the derived equations will be limited to small incident angles for the ultrasound beam.

After applying the Kirchoff-Helmholtz integral theorem, the pressure field is given by [*Pierce*, 1991]

$$p_{plane}(\vec{r}_d,\omega)=\frac{1}{4\pi}\iint_{S_f} d\vec{r}_f\vec{n}_f\cdot\left(g(\vec{r}_d,\vec{r}_f)\nabla_f p_{plane}(\vec{r}_f,\omega)-p_{plane}(\vec{r}_f,\omega)\nabla_f g(\vec{r}_d,\vec{r}_f)\right), \qquad \text{(G.3)}$$

which, after applying the appropriate Green's function g, becomes [*Pierce*, 1991]

$$p_{plane}(\vec{r}_d,\omega)=\frac{1}{2\pi}\iint_{S_f} d\vec{r}_f\vec{n}_f\cdot\left(\frac{e^{i\tilde{k}|\vec{r}_d-\vec{r}_f|}}{|\vec{r}_d-\vec{r}_f|}\nabla_f p_{plane}(\vec{r}_f,\omega)\right). \qquad \text{(G.4)}$$

Hence, it is the pressure field immediately after it reflects from the planar surface (i.e. $p_{plane}(\vec{r}_f,\omega)$) that needs to be determined.

In order to find the pressure field after reflection, an appropriate image source will be generated and the field from the image source will be determined at the plane. Before continuing the assumptions involved with using an image source for this problem need to be discussed. Image sources are normally used to quickly satisfy the boundary conditions of either pressure release or rigid surfaces. Hence, the use of image sources assumes that the impedance of the plate is very different from the impedance of the fluid surrounding the plate.

The location of the image source can be found by reflecting the original source across the plane. The reflection of an arbitrary point (x,y,z) across a plane is given by [*Hearn and Baker*, 1997]

$$\begin{bmatrix}x_I\\y_I\\z_I\\1\end{bmatrix}=\overbrace{\begin{bmatrix}1&0&0&0\\0&1&0&0\\0&0&1&z_p\\0&0&0&1\end{bmatrix}}^{Translation}\overbrace{\begin{bmatrix}-\cos(\phi_f)&\sin(\phi_f)&0&0\\-\sin(\phi_f)&-\cos(\phi_f)&0&0\\0&0&1&0\\0&0&0&1\end{bmatrix}}^{\phi-Rotation}\overbrace{\begin{bmatrix}-\cos(\theta_f)&0&-\sin(\theta_f)&0\\0&1&0&0\\\sin(\theta_f)&0&-\cos(\theta_f)&0\\0&0&0&1\end{bmatrix}}^{\theta-Rotation}$$

$$\overbrace{\begin{bmatrix}1&0&0&0\\0&1&0&0\\0&0&-1&0\\0&0&0&1\end{bmatrix}}^{Reflection}\overbrace{\begin{bmatrix}-\cos(\theta_f)&0&\sin(\theta_f)&0\\0&1&0&0\\-\sin(\theta_f)&0&-\cos(\theta_f)&0\\0&0&0&1\end{bmatrix}}^{\theta-Rotation}\overbrace{\begin{bmatrix}-\cos(\phi_f)&-\sin(\phi_f)&0&0\\\sin(\phi_f)&-\cos(\phi_f)&0&0\\0&0&1&0\\0&0&0&1\end{bmatrix}}^{\phi-Rotation}\overbrace{\begin{bmatrix}1&0&0&0\\0&1&0&0\\0&0&1&-z_p\\0&0&0&1\end{bmatrix}}^{Translation}\begin{bmatrix}x\\y\\z\\1\end{bmatrix}$$

$$
= \begin{bmatrix} 1 & 0 & 0 & 0 \\ 0 & 1 & 0 & 0 \\ 0 & 0 & 1 & z_p \\ 0 & 0 & 0 & 1 \end{bmatrix} \begin{bmatrix} \cos(\phi_f)\cos(\theta_f) & \sin(\phi_f) & \sin(\theta_f)\cos(\phi_f) & 0 \\ \sin(\phi_f)\cos(\theta_f) & -\cos(\phi_f) & \sin(\theta_f)\sin(\phi_f) & 0 \\ \sin(\theta_f) & 0 & -\cos(\theta_f) & 0 \\ 0 & 0 & 0 & 1 \end{bmatrix} \begin{bmatrix} 1 & 0 & 0 & 0 \\ 0 & 1 & 0 & 0 \\ 0 & 0 & -1 & 0 \\ 0 & 0 & 0 & 1 \end{bmatrix}
$$

$$
\begin{bmatrix} \cos(\phi_f)\cos(\theta_f) & \sin(\phi_f)\cos(\theta_f) & \sin(\theta_f) & 0 \\ \sin(\phi_f) & -\cos(\phi_f) & 0 & 0 \\ \sin(\theta_f)\cos(\phi_f) & \sin(\theta_f)\sin(\phi_f) & -\cos(\theta_f) & 0 \\ 0 & 0 & 0 & 1 \end{bmatrix} \begin{bmatrix} 1 & 0 & 0 & 0 \\ 0 & 1 & 0 & 0 \\ 0 & 0 & 1 & -z_p \\ 0 & 0 & 0 & 1 \end{bmatrix} \begin{bmatrix} x \\ y \\ z \\ 1 \end{bmatrix}
$$

$$
= \begin{bmatrix} \left(1-2\sin^2(\theta_f)\cos^2(\phi_f)\right) & -2\sin^2(\theta_f)\sin(\phi_f)\cos(\phi_f) & 2\sin(\theta_f)\cos(\phi_f)\cos(\theta_f) & 0 \\ -2\sin^2(\theta_f)\sin(\phi_f)\cos(\phi_f) & \left(1-2\sin^2(\theta_f)\sin^2(\phi_f)\right) & 2\sin(\theta_f)\sin(\phi_f)\cos(\theta_f) & 0 \\ 2\sin(\theta_f)\cos(\phi_f)\cos(\theta_f) & 2\sin(\theta_f)\sin(\phi_f)\cos(\theta_f) & \left(1-2\cos^2(\theta_f)\right) & z_p \\ 0 & 0 & 0 & 1 \end{bmatrix}
$$

$$
\begin{bmatrix} 1 & 0 & 0 & 0 \\ 0 & 1 & 0 & 0 \\ 0 & 0 & 1 & -z_p \\ 0 & 0 & 0 & 1 \end{bmatrix} \begin{bmatrix} x \\ y \\ z \\ 1 \end{bmatrix} = \begin{bmatrix} \mathbf{M}_{\mathbf{image}}^{1,1} & \mathbf{M}_{\mathbf{image}}^{1,2} & \mathbf{M}_{\mathbf{image}}^{1,3} & \mathbf{M}_{\mathbf{image}}^{1,4} \\ \mathbf{M}_{\mathbf{image}}^{2,1} & \mathbf{M}_{\mathbf{image}}^{2,2} & \mathbf{M}_{\mathbf{image}}^{2,3} & \mathbf{M}_{\mathbf{image}}^{2,4} \\ \mathbf{M}_{\mathbf{image}}^{3,1} & \mathbf{M}_{\mathbf{image}}^{3,2} & \mathbf{M}_{\mathbf{image}}^{3,3} & \mathbf{M}_{\mathbf{image}}^{3,4} \\ 0 & 0 & 0 & 1 \end{bmatrix} \begin{bmatrix} x \\ y \\ z \\ 1 \end{bmatrix} = \mathbf{M}_{\mathbf{image}} \begin{bmatrix} x \\ y \\ z \\ 1 \end{bmatrix},
$$

(G.5)

where

$$
\mathbf{M}_{\mathbf{image}}(:,1) = \begin{bmatrix} \left(1-2\sin^2(\theta_f)\cos^2(\phi_f)\right) \\ -2\sin^2(\theta_f)\sin(\phi_f)\cos(\phi_f) \\ 2\sin(\theta_f)\cos(\phi_f)\cos(\theta_f) \\ 0 \end{bmatrix} \quad \mathbf{M}_{\mathbf{image}}(:,2) = \begin{bmatrix} -2\sin^2(\theta_f)\sin(\phi_f)\cos(\phi_f) \\ \left(1-2\sin^2(\theta_f)\sin^2(\phi_f)\right) \\ 2\sin(\theta_f)\sin(\phi_f)\cos(\theta_f) \\ 0 \end{bmatrix}
$$

$$
\mathbf{M}_{\mathbf{image}}(:,3) = \begin{bmatrix} 2\sin(\theta_f)\cos(\phi_f)\cos(\theta_f) \\ 2\sin(\theta_f)\sin(\phi_f)\cos(\theta_f) \\ \left(1-2\cos^2(\theta_f)\right) \\ 0 \end{bmatrix} \quad \mathbf{M}_{\mathbf{image}}(:,4) = \begin{bmatrix} -2z_p\sin(\theta_f)\cos(\phi_f)\cos(\theta_f) \\ -2z_p\sin(\theta_f)\sin(\phi_f)\cos(\theta_f) \\ 2z_p\cos^2(\theta_f) \\ 1 \end{bmatrix}
$$

(G.6)

and (x_I, y_I, z_I) is the image of the original point. Therefore, the field from the image source would be given by [*Pierce*, 1991]

$$p_{plane}\left(\vec{r}_f,\omega\right)=\frac{-1}{2\pi}\iint_{S_I} d\vec{r}_I\vec{n}_I\cdot\left(\frac{e^{i\tilde{k}\left|\vec{r}_I-\vec{r}_f\right|}}{\left|\vec{r}_I-\vec{r}_f\right|}\nabla_I p_{plane}\left(\vec{r}_I,\omega\right)\right)=\frac{-i\omega\rho}{2\pi}\iint_{S_I} d\vec{r}_I\vec{n}_I\cdot\left(\frac{e^{i\tilde{k}\left|\vec{r}_I-\vec{r}_f\right|}}{\left|\vec{r}_I-\vec{r}_f\right|}\vec{u}\left(\vec{r}_I,\omega\right)\right)$$
$$=\frac{-i\omega\rho\Gamma_{plane}K_{uV}\left(\omega\right)V_{inc}\left(\omega\right)H\left(\omega\right)}{2\pi}\iint_{S_I} d\vec{r}_I G_T\left(\vec{r}_I,\omega\right)\frac{e^{i\tilde{k}\left|\vec{r}_I-\vec{r}_f\right|}}{\left|\vec{r}_I-\vec{r}_f\right|}, \tag{G.7}$$

where Γ_{plane} accounts for the fact that the plane may not be a perfect reflector, and $\vec{n}_I$ is the normal vector perpendicular to the aperture plane of the image source pointing away from the direction of wave propagation. Note that Γ_{plane} is only intended to correct for small deviations from a perfect reflector. Large deviations are not allowed under the current method of images formulation. Also, assuming that the planar surface is near the focus (i.e., $\left|\vec{r}_f\right|$ is small compared to $\left|\vec{r}_I\right|$), Equation (G.7) becomes

$$p_{plane}\left(\vec{r}_f,\omega\right)\cong\frac{-i\omega\rho\Gamma_{plane}K_{uV}\left(\omega\right)V_{inc}\left(\omega\right)H\left(\omega\right)}{2\pi}\iint_{S_I} d\vec{r}_I G_T\left(\vec{r}_I,\omega\right)\frac{e^{i\tilde{k}r_I}}{r_I}e^{-i\tilde{k}\frac{\vec{r}_I\cdot\vec{r}_f}{r_I}}, \tag{G.8}$$

which can be written in closed form if the velocity potential field near the focus can be approximated as a three-dimensional Gaussian. Hence, Equation (G.8) becomes

$$p_{plane}\left(\vec{r}_f,\omega\right)\cong\frac{-i\omega\rho\Gamma_{plane}K_{uV}\left(\omega\right)V_{inc}\left(\omega\right)H\left(\omega\right)G_o}{2\pi}e^{-\left(\left(\frac{\xi_x}{w_x}\right)^2+\left(\frac{\xi_y}{w_y}\right)^2+\left(\frac{\xi_z}{w_z}\right)^2\right)}e^{i\tilde{k}\left(z_T-\xi_z\right)}, \tag{G.9}$$

where $\left(\xi_x,\xi_y,\xi_z\right)$ refer to the coordinate system for the image source and z_T is also the distance of the aperture plane of the image source from its focus (same as for the original source).

The locations of points $\left(\xi_x,\xi_y,\xi_z\right)$ now need to be determined in the original coordinate system. Because the ξ_x-axis, ξ_y-axis, and ξ_z-axis are the image of the x-axis, y-axis, and z-axis, Equation (G.5) yields

$$\begin{array}{lll}\hat{\xi}_x\cdot\hat{x}=\mathbf{M}_{\mathbf{image}}^{1,1} & \hat{\xi}_y\cdot\hat{x}=\mathbf{M}_{\mathbf{image}}^{1,2} & \hat{\xi}_z\cdot\hat{x}=\mathbf{M}_{\mathbf{image}}^{1,3}\\ \hat{\xi}_x\cdot\hat{y}=\mathbf{M}_{\mathbf{image}}^{2,1} & \hat{\xi}_y\cdot\hat{y}=\mathbf{M}_{\mathbf{image}}^{2,2} & \hat{\xi}_z\cdot\hat{y}=\mathbf{M}_{\mathbf{image}}^{2,3}\\ \hat{\xi}_x\cdot\hat{z}=\mathbf{M}_{\mathbf{image}}^{3,1} & \hat{\xi}_y\cdot\hat{z}=\mathbf{M}_{\mathbf{image}}^{2,3} & \hat{\xi}_z\cdot\hat{z}=\mathbf{M}_{\mathbf{image}}^{3,3}\end{array}, \tag{G.10}$$

and the origin of the $\left(\xi_x,\xi_y,\xi_z\right)$ coordinate system is located at $\left(\mathbf{M}_{\mathbf{image}}^{1,4},\mathbf{M}_{\mathbf{image}}^{2,4},\mathbf{M}_{\mathbf{image}}^{3,4}\right)$. Therefore, $\left(\xi_x,\xi_y,\xi_z\right)$ in $\left(x,y,z\right)$ coordinates are given by

$$\begin{aligned}\xi_x &= x\mathbf{M}^{1,1}_{\mathbf{image}} + y\mathbf{M}^{2,1}_{\mathbf{image}} + z\mathbf{M}^{3,1}_{\mathbf{image}} + \mathbf{M}^{1,4}_{\mathbf{image}} \\ \xi_y &= x\mathbf{M}^{1,2}_{\mathbf{image}} + y\mathbf{M}^{2,2}_{\mathbf{image}} + z\mathbf{M}^{3,2}_{\mathbf{image}} + \mathbf{M}^{2,4}_{\mathbf{image}} \\ \xi_z &= x\mathbf{M}^{1,3}_{\mathbf{image}} + y\mathbf{M}^{2,3}_{\mathbf{image}} + z\mathbf{M}^{3,3}_{\mathbf{image}} + \mathbf{M}^{3,4}_{\mathbf{image}}\end{aligned} \tag{G.11}$$

providing an expression for $p_{plane}\left(\vec{r}_f,\omega\right)$ in closed form.

Now determine $\vec{n}_f \cdot \nabla_f p_{plane}\left(\vec{r}_f,\omega\right)$ by taking the gradient of Equation (G.9) to yield

$$\begin{aligned}\nabla_f p_{plane}\left(\vec{r}_f,\omega\right) &\cong \frac{-i\omega\rho\Gamma_{plane}K_{uV}(\omega)V_{inc}(\omega)H(\omega)G_o}{2\pi}\nabla_f\left(e^{-\left(\left(\frac{\xi_x}{w_x}\right)^2+\left(\frac{\xi_y}{w_y}\right)^2+\left(\frac{\xi_z}{w_z}\right)^2\right)}e^{i\tilde{k}\left(z_T-\xi_z\right)}\right) \\ &= \frac{-i\omega\rho\Gamma_{plane}K_{uV}(\omega)V_{inc}(\omega)H(\omega)G_o}{2\pi}\left(e^{-\left(\left(\frac{\xi_x}{w_x}\right)^2+\left(\frac{\xi_y}{w_y}\right)^2+\left(\frac{\xi_z}{w_z}\right)^2\right)}e^{i\tilde{k}\left(z_T-\xi_z\right)}\right) \\ &\quad \nabla_f\left(i\tilde{k}\left(z_T-\xi_z\right)-\left(\left(\frac{\xi_x}{w_x}\right)^2+\left(\frac{\xi_y}{w_y}\right)^2+\left(\frac{\xi_z}{w_z}\right)^2\right)\right) \\ &= \frac{i\omega\rho\Gamma_{plane}K_{uV}(\omega)V_{inc}(\omega)H(\omega)G_o}{2\pi}\left(e^{-\left(\left(\frac{\xi_x}{w_x}\right)^2+\left(\frac{\xi_y}{w_y}\right)^2+\left(\frac{\xi_z}{w_z}\right)^2\right)}e^{i\tilde{k}\left(z_T-\xi_z\right)}\right) \\ &\quad \nabla_f\left(i\tilde{k}\xi_z+\left(\frac{\xi_x}{w_x}\right)^2+\left(\frac{\xi_y}{w_y}\right)^2+\left(\frac{\xi_z}{w_z}\right)^2\right) \\ &= \frac{i\omega\rho\Gamma_{plane}K_{uV}(\omega)V_{inc}(\omega)H(\omega)G_o}{2\pi}\left(e^{-\left(\left(\frac{\xi_x}{w_x}\right)^2+\left(\frac{\xi_y}{w_y}\right)^2+\left(\frac{\xi_z}{w_z}\right)^2\right)}e^{i\tilde{k}\left(z_T-\xi_z\right)}\right) \\ &\quad \left(i\tilde{k}\nabla_f\xi_z+2\frac{\xi_x}{w_x}\nabla_f\xi_x+2\frac{\xi_y}{w_y}\nabla_f\xi_y+2\frac{\xi_z}{w_z}\nabla_f\xi_z\right).\end{aligned} \tag{G.12}$$

Now taking the derivative of the expressions given in Equation (G.11) for ξ_x, ξ_y, and ξ_z yields

$$\nabla_f\xi_x = \begin{bmatrix}\mathbf{M}^{1,1}_{\mathbf{image}} \\ \mathbf{M}^{2,1}_{\mathbf{image}} \\ \mathbf{M}^{3,1}_{\mathbf{image}}\end{bmatrix} \quad \nabla_f\xi_y = \begin{bmatrix}\mathbf{M}^{1,2}_{\mathbf{image}} \\ \mathbf{M}^{2,2}_{\mathbf{image}} \\ \mathbf{M}^{3,2}_{\mathbf{image}}\end{bmatrix} \quad \nabla_f\xi_z = \begin{bmatrix}\mathbf{M}^{1,3}_{\mathbf{image}} \\ \mathbf{M}^{2,3}_{\mathbf{image}} \\ \mathbf{M}^{3,3}_{\mathbf{image}}\end{bmatrix}. \tag{G.13}$$

Also, taking the dot product of the expressions in Equation (G.13) with $\vec{n}_f$ yields

$$\vec{n}_f \cdot \nabla_f \xi_x = \mathbf{M}^{1,1}_{\mathbf{image}} \sin(\theta_f)\cos(\phi_f) + \mathbf{M}^{2,1}_{\mathbf{image}} \sin(\theta_f)\sin(\phi_f) - \mathbf{M}^{3,1}_{\mathbf{image}} \cos(\theta_f)$$
$$\vec{n}_f \cdot \nabla_f \xi_y = \mathbf{M}^{1,2}_{\mathbf{image}} \sin(\theta_f)\cos(\phi_f) + \mathbf{M}^{2,2}_{\mathbf{image}} \sin(\theta_f)\sin(\phi_f) - \mathbf{M}^{3,2}_{\mathbf{image}} \cos(\theta_f) \qquad \text{(G.14)}$$
$$\vec{n}_f \cdot \nabla_f \xi_z = \mathbf{M}^{1,3}_{\mathbf{image}} \sin(\theta_f)\cos(\phi_f) + \mathbf{M}^{2,3}_{\mathbf{image}} \sin(\theta_f)\sin(\phi_f) - \mathbf{M}^{3,3}_{\mathbf{image}} \cos(\theta_f).$$

At this point, the results can be simplified by assuming that θ_f is less than $\pi/6$, the typical critical angle for longitudinal waves going from tissue to bone [*Fujii et al.*, 1999]. Larger angles would result in no signal entering the brain and, consequently, no image of the brain could be formed. Also, a small incident angle is required if the neglecting of shear waves is going to be valid [*Mayer*, 1964]. Under this assumption, $2\frac{\xi_x}{w_x}\nabla_f \xi_x$, $2\frac{\xi_y}{w_y}\nabla_f \xi_y$, and $2\frac{\xi_z}{w_z}\nabla_f \xi_z$ are all small compared to $i\tilde{k}\nabla_f \xi_z$. Hence, $\vec{n}_f \cdot \nabla_f p_{plane}(\vec{r}_f, \omega)$ can be approximated as

$$\vec{n}_f \cdot \nabla_f p_{plane}(\vec{r}_f, \omega) \cong \frac{-\tilde{k}\,\omega\rho\Gamma_{plane} K_{uV}(\omega) V_{inc}(\omega) H(\omega) G_o}{2\pi} \left(e^{-\left(\left(\frac{\xi_x}{w_x}\right)^2 + \left(\frac{\xi_y}{w_y}\right)^2 + \left(\frac{\xi_z}{w_z}\right)^2\right)} e^{i\tilde{k}(z_T - \xi_z)} \right) (\vec{n}_f \cdot \nabla_f \xi_z)$$

$$= \frac{-\tilde{k}\,\omega\rho\Gamma_{plane} K_{uV}(\omega) V_{inc}(\omega) H(\omega) G_o}{2\pi} \left(e^{-\left(\left(\frac{\xi_x}{w_x}\right)^2 + \left(\frac{\xi_y}{w_y}\right)^2 + \left(\frac{\xi_z}{w_z}\right)^2\right)} e^{i\tilde{k}(z_T - \xi_z)} \right) \cos(\theta_f). \quad \text{(G.15)}$$

Now that an expression for $\vec{n}_f \cdot \nabla_f p_{plane}(\vec{r}_f, \omega)$ has been derived, $p_{plane}(\vec{r}_d, \omega)$ can be found from Equation (G.4). Substituting in for the necessary parameters yields

$$p_{plane}(\vec{r}_d, \omega) = \frac{1}{2\pi} \iint_{S_f} d\vec{r}_f \, \frac{e^{i\tilde{k}|\vec{r}_d - \vec{r}_f|}}{|\vec{r}_d - \vec{r}_f|} \left(\vec{n}_f \cdot \nabla_f p_{plane}(\vec{r}_f, \omega)\right)$$

$$= \frac{-\tilde{k}\,\omega\rho\Gamma_{plane} K_{uV}(\omega) V_{inc}(\omega) H(\omega) G_o \cos(\theta_f)}{(2\pi)^2} \iint_{S_f} d\vec{r}_f \, \frac{e^{i\tilde{k}|\vec{r}_d - \vec{r}_f|}}{|\vec{r}_d - \vec{r}_f|} \left(e^{-\left(\left(\frac{\xi_x}{w_x}\right)^2 + \left(\frac{\xi_y}{w_y}\right)^2 + \left(\frac{\xi_z}{w_z}\right)^2\right)} e^{i\tilde{k}(z_T - \xi_z)} \right), \quad \text{(G.16)}$$

where ξ_x, ξ_y, and ξ_z are given by Equation (G.11).

After determining the reflected fields in the region containing the original ultrasound source, these fields need to be translated to a voltage output by the transducer. The voltage output by the source can be found from

$$V_{plane}(\omega) = \frac{H(\omega)}{i\omega\rho S_T K_{uV}(\omega)} \iint_{S_T} d\vec{r}_d \, G_T(\vec{r}_d, \omega) \frac{\partial p_{plane}}{\partial z_d}, \tag{G.17}$$

where $\partial p_{plane} / \partial z_d$ is given by

$$\begin{aligned}
\frac{\partial}{\partial z_d} p_{plane}(\vec{r}_d, \omega) &= \frac{-\tilde{k}\,\omega\rho\Gamma_{plane} K_{uV}(\omega) V_{inc}(\omega) H(\omega) G_o \cos(\theta_f)}{(2\pi)^2} \\
&\cdot \iint_{S_f} d\vec{r}_f \left(e^{-\left(\left(\frac{\xi_x}{w_x}\right)^2 + \left(\frac{\xi_y}{w_y}\right)^2 + \left(\frac{\xi_z}{w_z}\right)^2\right)} e^{i\tilde{k}(z_T - \xi_z)} \right) \frac{\partial}{\partial z_d} \frac{e^{i\tilde{k}|\vec{r}_d - \vec{r}_f|}}{|\vec{r}_d - \vec{r}_f|} \\
&\cong \frac{-\tilde{k}\,\omega\rho\Gamma_{plane} K_{uV}(\omega) V_{inc}(\omega) H(\omega) G_o \cos(\theta_f)}{(2\pi)^2} \\
&\cdot \iint_{S_f} d\vec{r}_f \left(e^{-\left(\left(\frac{\xi_x}{w_x}\right)^2 + \left(\frac{\xi_y}{w_y}\right)^2 + \left(\frac{\xi_z}{w_z}\right)^2\right)} e^{i\tilde{k}(z_T - \xi_z)} \right) \frac{i\tilde{k} z_d}{r_d^2} e^{i\tilde{k} r_d - i\tilde{k}\vec{r}_f \cdot \frac{\vec{r}_d}{r_d}} \\
&\cong \frac{-i\tilde{k}^2\,\omega\rho\Gamma_{plane} K_{uV}(\omega) V_{inc}(\omega) H(\omega) G_o \cos(\theta_f)}{(2\pi)^2} \\
&\cdot \iint_{S_f} d\vec{r}_f \left(e^{-\left(\left(\frac{\xi_x}{w_x}\right)^2 + \left(\frac{\xi_y}{w_y}\right)^2 + \left(\frac{\xi_z}{w_z}\right)^2\right)} e^{i\tilde{k}(z_T - \xi_z)} \right) \frac{e^{i\tilde{k} r_d - i\tilde{k}\vec{r}_f \cdot \frac{\vec{r}_d}{r_d}}}{r_d}.
\end{aligned} \tag{G.18}$$

Hence, the reflected voltage from the plate is given by

$$\begin{aligned}
V_{plane}(\omega) &\cong \frac{-\tilde{k}^2 \Gamma_{plane} V_{inc}(\omega) H^2(\omega) G_o \cos(\theta_f)}{S_T (2\pi)^2} \\
&\cdot \iint_{S_T} d\vec{r}_d G_T(\vec{r}_d, \omega) \iint_{S_f} d\vec{r}_f \left(e^{-\left(\left(\frac{\xi_x}{w_x}\right)^2 + \left(\frac{\xi_y}{w_y}\right)^2 + \left(\frac{\xi_z}{w_z}\right)^2\right)} e^{i\tilde{k}(z_T - \xi_z)} \right) \frac{e^{i\tilde{k} r_d - i\tilde{k}\vec{r}_f \cdot \frac{\vec{r}_d}{r_d}}}{r_d} \\
&= \frac{-\tilde{k}^2 \Gamma_{plane} V_{inc}(\omega) H^2(\omega) G_o \cos(\theta_f)}{S_T (2\pi)^2} \\
&\cdot \iint_{S_f} d\vec{r}_f \left(e^{-\left(\left(\frac{\xi_x}{w_x}\right)^2 + \left(\frac{\xi_y}{w_y}\right)^2 + \left(\frac{\xi_z}{w_z}\right)^2\right)} e^{i\tilde{k}(z_T - \xi_z)} \left(\iint_{S_T} d\vec{r}_d G_T(\vec{r}_d, \omega) \frac{e^{i\tilde{k} r_d - i\tilde{k}\vec{r}_f \cdot \frac{\vec{r}_d}{r_d}}}{r_d} \right) \right)
\end{aligned}$$

$$= \frac{-\tilde{k}^2 \Gamma_{plane} V_{inc}(\omega) H^2(\omega) G_o^2 \cos(\theta_f)}{S_T (2\pi)^2}$$

$$\cdot \iint_{S_f} d\vec{r}_f \left(e^{-\left(\left(\frac{\xi_x}{w_x}\right)^2 + \left(\frac{\xi_y}{w_y}\right)^2 + \left(\frac{\xi_z}{w_z}\right)^2\right)} e^{i\tilde{k}(z_T - \xi_z)} \left(e^{-\left(\left(\frac{x_f}{w_x}\right)^2 + \left(\frac{y_f}{w_y}\right)^2 + \left(\frac{z_f}{w_z}\right)^2\right)} e^{i\tilde{k}(z_T - z_f)} \right) \right)$$

$$= \Omega(\omega) \iint_{S_f} d\vec{r}_f \left(e^{-\left(\frac{\xi_x^2 + x_f^2}{w_x^2} + \frac{\xi_y^2 + y_f^2}{w_y^2} + \frac{\xi_z^2 + z_f^2}{w_z^2} + i\tilde{k}(\xi_z + z_f)\right)} \right), \tag{G.19}$$

where the velocity potential fields has been assumed to be Gaussian and $\Omega(\omega)$ is given by

$$\Omega(\omega) = \frac{-\tilde{k}^2 \Gamma_{plane} V_{inc}(\omega) H^2(\omega) G_o^2 \cos(\theta_f)}{S_T (2\pi)^2} e^{i2\tilde{k} z_T}. \tag{G.20}$$

In order to integrate Equation (G.19), all of the spatial coordinates need to be expressed in terms of x_f and y_f. Solving Equations (G.11) and (G.2) yields

$$\begin{aligned}
\xi_x^2 &= x_f^2 \mathbf{M}_{\mathbf{image}}^{1,1} \mathbf{M}_{\mathbf{image}}^{1,1} + y_f^2 \mathbf{M}_{\mathbf{image}}^{2,1} \mathbf{M}_{\mathbf{image}}^{2,1} + z_f^2 \mathbf{M}_{\mathbf{image}}^{3,1} \mathbf{M}_{\mathbf{image}}^{3,1} + \mathbf{M}_{\mathbf{image}}^{1,4} \mathbf{M}_{\mathbf{image}}^{1,4} \\
&\quad + 2x_f y_f \mathbf{M}_{\mathbf{image}}^{1,1} \mathbf{M}_{\mathbf{image}}^{2,1} + 2x_f z_f \mathbf{M}_{\mathbf{image}}^{1,1} \mathbf{M}_{\mathbf{image}}^{3,1} + 2x_f \mathbf{M}_{\mathbf{image}}^{1,1} \mathbf{M}_{\mathbf{image}}^{1,4} + 2y_f z_f \mathbf{M}_{\mathbf{image}}^{2,1} \mathbf{M}_{\mathbf{image}}^{3,1} \\
&\quad + 2y_f \mathbf{M}_{\mathbf{image}}^{2,1} \mathbf{M}_{\mathbf{image}}^{1,4} + 2z_f \mathbf{M}_{\mathbf{image}}^{3,1} \mathbf{M}_{\mathbf{image}}^{1,4} \\
\xi_y^2 &= x_f^2 \mathbf{M}_{\mathbf{image}}^{1,2} \mathbf{M}_{\mathbf{image}}^{1,2} + y_f^2 \mathbf{M}_{\mathbf{image}}^{2,2} \mathbf{M}_{\mathbf{image}}^{2,2} + z_f^2 \mathbf{M}_{\mathbf{image}}^{3,2} \mathbf{M}_{\mathbf{image}}^{3,2} + \mathbf{M}_{\mathbf{image}}^{2,4} \mathbf{M}_{\mathbf{image}}^{2,4} \\
&\quad + 2x_f y_f \mathbf{M}_{\mathbf{image}}^{1,2} \mathbf{M}_{\mathbf{image}}^{2,2} + 2x_f z_f \mathbf{M}_{\mathbf{image}}^{1,2} \mathbf{M}_{\mathbf{image}}^{3,2} + 2x_f \mathbf{M}_{\mathbf{image}}^{1,2} \mathbf{M}_{\mathbf{image}}^{2,4} + 2y_f z_f \mathbf{M}_{\mathbf{image}}^{2,2} \mathbf{M}_{\mathbf{image}}^{3,2} \\
&\quad + 2y_f \mathbf{M}_{\mathbf{image}}^{2,2} \mathbf{M}_{\mathbf{image}}^{2,4} + 2z_f \mathbf{M}_{\mathbf{image}}^{3,2} \mathbf{M}_{\mathbf{image}}^{2,4} \\
\xi_z^2 &= x_f^2 \mathbf{M}_{\mathbf{image}}^{1,3} \mathbf{M}_{\mathbf{image}}^{1,3} + y_f^2 \mathbf{M}_{\mathbf{image}}^{2,3} \mathbf{M}_{\mathbf{image}}^{2,3} + z_f^2 \mathbf{M}_{\mathbf{image}}^{3,3} \mathbf{M}_{\mathbf{image}}^{3,3} + \mathbf{M}_{\mathbf{image}}^{3,4} \mathbf{M}_{\mathbf{image}}^{3,4} \\
&\quad + 2x_f y_f \mathbf{M}_{\mathbf{image}}^{1,3} \mathbf{M}_{\mathbf{image}}^{2,3} + 2x_f z_f \mathbf{M}_{\mathbf{image}}^{1,3} \mathbf{M}_{\mathbf{image}}^{3,3} + 2x_f \mathbf{M}_{\mathbf{image}}^{1,3} \mathbf{M}_{\mathbf{image}}^{3,4} + 2y_f z_f \mathbf{M}_{\mathbf{image}}^{2,3} \mathbf{M}_{\mathbf{image}}^{3,3} \\
&\quad + 2y_f \mathbf{M}_{\mathbf{image}}^{2,3} \mathbf{M}_{\mathbf{image}}^{3,4} + 2z_f \mathbf{M}_{\mathbf{image}}^{3,3} \mathbf{M}_{\mathbf{image}}^{3,4}
\end{aligned} \tag{G.21}$$

and

$$\begin{aligned}
z_f &= x_f \cdot \tan(\theta_f) \cos(\phi_f) + y_f \cdot \tan(\theta_f) \sin(\phi_f) + z_p \\
&= x_f C_1 + y_f C_2 + z_p \\
\Rightarrow z_f^2 &= x_f^2 C_1^2 + 2x_f y_f C_1 C_2 + 2x_f z_p C_1 + y_f^2 C_2^2 + 2y_f z_p C_2 + z_p^2,
\end{aligned} \tag{G.22}$$

where

$$\begin{aligned}
C_1 &= \tan(\theta_f) \cos(\phi_f) \\
C_2 &= \tan(\theta_f) \sin(\phi_f).
\end{aligned} \tag{G.23}$$

Now consider each term of the exponent of Equation (G.19) individually.

$$i\tilde{k}\left(\xi_z + z_f\right) = i\tilde{k}\left(\begin{array}{l} x_f\left(\mathbf{M}^{1,3}_{\mathbf{image}} + C_1 + C_1\mathbf{M}^{3,3}_{\mathbf{image}}\right) + y_f\left(\mathbf{M}^{2,3}_{\mathbf{image}} + C_2 + C_2\mathbf{M}^{3,3}_{\mathbf{image}}\right) \\ +\mathbf{M}^{3,4}_{\mathbf{image}} + z_p\mathbf{M}^{3,3}_{\mathbf{image}} + z_p \end{array}\right) \quad \text{(G.24)}$$

$$\begin{aligned} \frac{\xi_x^2 + x_f^2}{w_x^2} = {} & x_f^2\left(\frac{1}{w_x^2} + \frac{\mathbf{M}^{1,1}_{\mathbf{image}}\mathbf{M}^{1,1}_{\mathbf{image}}}{w_x^2} + C_1^2\frac{\mathbf{M}^{3,1}_{\mathbf{image}}\mathbf{M}^{3,1}_{\mathbf{image}}}{w_x^2} + 2C_1\frac{\mathbf{M}^{1,1}_{\mathbf{image}}\mathbf{M}^{3,1}_{\mathbf{image}}}{w_x^2}\right) \\ & + x_f\left(\begin{array}{l} 2\frac{\mathbf{M}^{1,1}_{\mathbf{image}}\mathbf{M}^{1,4}_{\mathbf{image}}}{w_x^2} + 2z_pC_1\frac{\mathbf{M}^{3,1}_{\mathbf{image}}\mathbf{M}^{3,1}_{\mathbf{image}}}{w_x^2} + 2C_1\frac{\mathbf{M}^{3,1}_{\mathbf{image}}\mathbf{M}^{1,4}_{\mathbf{image}}}{w_x^2} \\ +2z_p\frac{\mathbf{M}^{1,1}_{\mathbf{image}}\mathbf{M}^{3,1}_{\mathbf{image}}}{w_x^2} \end{array}\right) \\ & + \left(\frac{\mathbf{M}^{1,4}_{\mathbf{image}}\mathbf{M}^{1,4}_{\mathbf{image}}}{w_x^2} + z_p^2\frac{\mathbf{M}^{3,1}_{\mathbf{image}}\mathbf{M}^{3,1}_{\mathbf{image}}}{w_x^2} + 2z_p\frac{\mathbf{M}^{3,1}_{\mathbf{image}}\mathbf{M}^{1,4}_{\mathbf{image}}}{w_x^2}\right) \\ & + y_f^2\left(\frac{\mathbf{M}^{2,1}_{\mathbf{image}}\mathbf{M}^{2,1}_{\mathbf{image}}}{w_x^2} + C_2^2\frac{\mathbf{M}^{3,1}_{\mathbf{image}}\mathbf{M}^{3,1}_{\mathbf{image}}}{w_x^2} + 2C_2\frac{\mathbf{M}^{2,1}_{\mathbf{image}}\mathbf{M}^{3,1}_{\mathbf{image}}}{w_x^2}\right) \\ & + y_f\left(\begin{array}{l} 2x_f\frac{\mathbf{M}^{1,1}_{\mathbf{image}}\mathbf{M}^{2,1}_{\mathbf{image}}}{w_x^2} + 2\frac{\mathbf{M}^{2,1}_{\mathbf{image}}\mathbf{M}^{1,4}_{\mathbf{image}}}{w_x^2} + 2x_fC_1C_2\frac{\mathbf{M}^{3,1}_{\mathbf{image}}\mathbf{M}^{3,1}_{\mathbf{image}}}{w_x^2} \\ +2z_pC_2\frac{\mathbf{M}^{3,1}_{\mathbf{image}}\mathbf{M}^{3,1}_{\mathbf{image}}}{w_x^2} + 2x_fC_1\frac{\mathbf{M}^{2,1}_{\mathbf{image}}\mathbf{M}^{3,1}_{\mathbf{image}}}{w_x^2} + 2x_fC_2\frac{\mathbf{M}^{1,1}_{\mathbf{image}}\mathbf{M}^{3,1}_{\mathbf{image}}}{w_x^2} \\ +2C_2\frac{\mathbf{M}^{3,1}_{\mathbf{image}}\mathbf{M}^{1,4}_{\mathbf{image}}}{w_x^2} + 2z_p\frac{\mathbf{M}^{2,1}_{\mathbf{image}}\mathbf{M}^{3,1}_{\mathbf{image}}}{w_x^2} \end{array}\right) \end{aligned} \quad \text{(G.25)}$$

$$\begin{aligned} \frac{\xi_y^2 + y_f^2}{w_y^2} = {} & x_f^2\left(\frac{\mathbf{M}^{1,2}_{\mathbf{image}}\mathbf{M}^{1,2}_{\mathbf{image}}}{w_y^2} + C_1^2\frac{\mathbf{M}^{3,2}_{\mathbf{image}}\mathbf{M}^{3,2}_{\mathbf{image}}}{w_y^2} + 2C_1\frac{\mathbf{M}^{1,2}_{\mathbf{image}}\mathbf{M}^{3,2}_{\mathbf{image}}}{w_y^2}\right) \\ & + x_f\left(\begin{array}{l} 2\frac{\mathbf{M}^{1,2}_{\mathbf{image}}\mathbf{M}^{2,4}_{\mathbf{image}}}{w_y^2} + 2z_pC_1\frac{\mathbf{M}^{3,2}_{\mathbf{image}}\mathbf{M}^{3,2}_{\mathbf{image}}}{w_y^2} + 2C_1\frac{\mathbf{M}^{3,2}_{\mathbf{image}}\mathbf{M}^{2,4}_{\mathbf{image}}}{w_y^2} \\ +2z_p\frac{\mathbf{M}^{1,2}_{\mathbf{image}}\mathbf{M}^{3,2}_{\mathbf{image}}}{w_y^2} \end{array}\right) \\ & + \left(\frac{\mathbf{M}^{2,4}_{\mathbf{image}}\mathbf{M}^{2,4}_{\mathbf{image}}}{w_y^2} + z_p^2\frac{\mathbf{M}^{3,2}_{\mathbf{image}}\mathbf{M}^{3,2}_{\mathbf{image}}}{w_y^2} + 2z_p\frac{\mathbf{M}^{3,2}_{\mathbf{image}}\mathbf{M}^{2,4}_{\mathbf{image}}}{w_y^2}\right) \\ & + y_f^2\left(\frac{1}{w_y^2} + \frac{\mathbf{M}^{2,2}_{\mathbf{image}}\mathbf{M}^{2,2}_{\mathbf{image}}}{w_y^2} + C_2^2\frac{\mathbf{M}^{3,2}_{\mathbf{image}}\mathbf{M}^{3,2}_{\mathbf{image}}}{w_y^2} + 2C_2\frac{\mathbf{M}^{2,2}_{\mathbf{image}}\mathbf{M}^{3,2}_{\mathbf{image}}}{w_y^2}\right) \end{aligned}$$

$$+ y_f \left(\begin{array}{l} 2x_f \dfrac{\mathbf{M}_{\mathbf{image}}^{1,2}\mathbf{M}_{\mathbf{image}}^{2,2}}{w_y^2} + 2\dfrac{\mathbf{M}_{\mathbf{image}}^{2,2}\mathbf{M}_{\mathbf{image}}^{2,4}}{w_y^2} + 2x_f C_1 C_2 \dfrac{\mathbf{M}_{\mathbf{image}}^{3,2}\mathbf{M}_{\mathbf{image}}^{3,2}}{w_y^2} \\ +2z_p C_2 \dfrac{\mathbf{M}_{\mathbf{image}}^{3,2}\mathbf{M}_{\mathbf{image}}^{3,2}}{w_y^2} + 2x_f C_1 \dfrac{\mathbf{M}_{\mathbf{image}}^{2,2}\mathbf{M}_{\mathbf{image}}^{3,2}}{w_y^2} + 2x_f C_2 \dfrac{\mathbf{M}_{\mathbf{image}}^{1,2}\mathbf{M}_{\mathbf{image}}^{3,2}}{w_y^2} \\ +2C_2 \dfrac{\mathbf{M}_{\mathbf{image}}^{3,2}\mathbf{M}_{\mathbf{image}}^{2,4}}{w_y^2} + 2z_p \dfrac{\mathbf{M}_{\mathbf{image}}^{2,2}\mathbf{M}_{\mathbf{image}}^{3,2}}{w_y^2} \end{array} \right)$$

(G.26)

$$\frac{\xi_z^2 + z_f^2}{w_z^2} = x_f^2 \left(\frac{\mathbf{M}_{\mathbf{image}}^{1,3}\mathbf{M}_{\mathbf{image}}^{1,3}}{w_z^2} + \frac{C_1^2}{w_z^2} + C_1^2 \frac{\mathbf{M}_{\mathbf{image}}^{3,3}\mathbf{M}_{\mathbf{image}}^{3,3}}{w_z^2} + 2C_1 \frac{\mathbf{M}_{\mathbf{image}}^{1,3}\mathbf{M}_{\mathbf{image}}^{3,3}}{w_z^2} \right)$$

$$+ x_f \left(\begin{array}{l} 2\dfrac{\mathbf{M}_{\mathbf{image}}^{1,3}\mathbf{M}_{\mathbf{image}}^{3,4}}{w_z^2} + \dfrac{2z_p C_1}{w_z^2} + 2z_p C_1 \dfrac{\mathbf{M}_{\mathbf{image}}^{3,3}\mathbf{M}_{\mathbf{image}}^{3,3}}{w_z^2} \\ +2C_1 \dfrac{\mathbf{M}_{\mathbf{image}}^{3,3}\mathbf{M}_{\mathbf{image}}^{3,4}}{w_z^2} + 2z_p \dfrac{\mathbf{M}_{\mathbf{image}}^{1,3}\mathbf{M}_{\mathbf{image}}^{3,3}}{w_z^2} \end{array} \right)$$

$$+ \left(\frac{\mathbf{M}_{\mathbf{image}}^{3,4}\mathbf{M}_{\mathbf{image}}^{3,4}}{w_z^2} + \frac{z_p^2}{w_z^2} + z_p^2 \frac{\mathbf{M}_{\mathbf{image}}^{3,3}\mathbf{M}_{\mathbf{image}}^{3,3}}{w_z^2} + 2z_p \frac{\mathbf{M}_{\mathbf{image}}^{3,3}\mathbf{M}_{\mathbf{image}}^{3,4}}{w_z^2} \right)$$

$$+ y_f^2 \left(\frac{\mathbf{M}_{\mathbf{image}}^{2,3}\mathbf{M}_{\mathbf{image}}^{2,3}}{w_z^2} + \frac{C_2^2}{w_z^2} + C_2^2 \frac{\mathbf{M}_{\mathbf{image}}^{3,3}\mathbf{M}_{\mathbf{image}}^{3,3}}{w_z^2} + 2C_2 \frac{\mathbf{M}_{\mathbf{image}}^{2,3}\mathbf{M}_{\mathbf{image}}^{3,3}}{w_z^2} \right)$$

$$+ y_f \left(\begin{array}{l} 2x_f \dfrac{\mathbf{M}_{\mathbf{image}}^{1,3}\mathbf{M}_{\mathbf{image}}^{2,3}}{w_z^2} + 2\dfrac{\mathbf{M}_{\mathbf{image}}^{2,3}\mathbf{M}_{\mathbf{image}}^{3,4}}{w_z^2} + \dfrac{2x_f C_1 C_2}{w_z^2} \\ +2x_f C_1 C_2 \dfrac{\mathbf{M}_{\mathbf{image}}^{3,3}\mathbf{M}_{\mathbf{image}}^{3,3}}{w_z^2} + \dfrac{2z_p C_2}{w_z^2} + 2z_p C_2 \dfrac{\mathbf{M}_{\mathbf{image}}^{3,3}\mathbf{M}_{\mathbf{image}}^{3,3}}{w_z^2} \\ +2x_f C_1 \dfrac{\mathbf{M}_{\mathbf{image}}^{2,3}\mathbf{M}_{\mathbf{image}}^{3,3}}{w_z^2} + 2x_f C_2 \dfrac{\mathbf{M}_{\mathbf{image}}^{1,3}\mathbf{M}_{\mathbf{image}}^{3,3}}{w_z^2} + 2C_2 \dfrac{\mathbf{M}_{\mathbf{image}}^{3,3}\mathbf{M}_{\mathbf{image}}^{3,4}}{w_z^2} \\ +2z_p \dfrac{\mathbf{M}_{\mathbf{image}}^{2,3}\mathbf{M}_{\mathbf{image}}^{3,3}}{w_z^2} \end{array} \right)$$

(G.27)

The appropriate terms can then be grouped resulting in an expression for the voltage returned from the plane given by

$$V_{plane}(\omega) \cong \Omega(\omega)\exp\left(-\left(\frac{C_x}{w_x^2}+\frac{C_y}{w_y^2}+\frac{C_z}{w_z^2}+i\tilde{k}C_k\right)\right)$$
$$\int_{-\infty}^{\infty} dx_f \left(\exp\left(\begin{array}{l}-x_f^2\left(\frac{X_{1x}}{w_x^2}+\frac{X_{1y}}{w_y^2}+\frac{X_{1z}}{w_z^2}\right)\\ -x_f\left(\frac{X_{2x}}{w_x^2}+\frac{X_{2y}}{w_y^2}+\frac{X_{2z}}{w_z^2}+i\tilde{k}X_k\right)\end{array}\right)\int_{-\infty}^{\infty} dy_f \exp\left(\begin{array}{l}-y_f^2\left(\frac{Y_{1x}}{w_x^2}+\frac{Y_{1y}}{w_y^2}+\frac{Y_{1z}}{w_z^2}\right)\\ -y_f\left(\frac{Y_{2x}}{w_x^2}+\frac{Y_{2y}}{w_y^2}+\frac{Y_{2z}}{w_z^2}\right)\\ +i\tilde{k}Y_k\end{array}\right)\right), \quad \text{(G.28)}$$

where

$$\begin{aligned} X_k &= \mathbf{M}_{\mathbf{image}}^{1,3} + C_1 + C_1\mathbf{M}_{\mathbf{image}}^{3,3} = 2\tan(\theta_f)\cos(\phi_f) \\ Y_k &= \mathbf{M}_{\mathbf{image}}^{2,3} + C_2 + C_2\mathbf{M}_{\mathbf{image}}^{3,3} = 2\tan(\theta_f)\sin(\phi_f) \\ C_k &= \mathbf{M}_{\mathbf{image}}^{3,4} + z_p\mathbf{M}_{\mathbf{image}}^{3,3} + z_p = 2z_p \end{aligned} \quad \text{(G.29)}$$

$$\begin{aligned} X_{1x} &= 1 + \mathbf{M}_{\mathbf{image}}^{1,1}\mathbf{M}_{\mathbf{image}}^{1,1} + C_1^2\mathbf{M}_{\mathbf{image}}^{3,1}\mathbf{M}_{\mathbf{image}}^{3,1} + 2C_1\mathbf{M}_{\mathbf{image}}^{1,1}\mathbf{M}_{\mathbf{image}}^{3,1} = 2 \\ X_{2x} &= 2\left(\mathbf{M}_{\mathbf{image}}^{1,1}\mathbf{M}_{\mathbf{image}}^{1,4} + z_pC_1\mathbf{M}_{\mathbf{image}}^{3,1}\mathbf{M}_{\mathbf{image}}^{3,1} + C_1\mathbf{M}_{\mathbf{image}}^{3,1}\mathbf{M}_{\mathbf{image}}^{1,4} + z_p\mathbf{M}_{\mathbf{image}}^{1,1}\mathbf{M}_{\mathbf{image}}^{3,1}\right) = 0 \end{aligned} \quad \text{(G.30)}$$

$$\begin{aligned} X_{1y} &= \mathbf{M}_{\mathbf{image}}^{1,2}\mathbf{M}_{\mathbf{image}}^{1,2} + C_1^2\mathbf{M}_{\mathbf{image}}^{3,2}\mathbf{M}_{\mathbf{image}}^{3,2} + 2C_1\mathbf{M}_{\mathbf{image}}^{1,2}\mathbf{M}_{\mathbf{image}}^{3,2} = 0 \\ X_{2y} &= 2\left(\mathbf{M}_{\mathbf{image}}^{1,2}\mathbf{M}_{\mathbf{image}}^{2,4} + z_pC_1\mathbf{M}_{\mathbf{image}}^{3,2}\mathbf{M}_{\mathbf{image}}^{3,2} + C_1\mathbf{M}_{\mathbf{image}}^{3,2}\mathbf{M}_{\mathbf{image}}^{2,4} + z_p\mathbf{M}_{\mathbf{image}}^{1,2}\mathbf{M}_{\mathbf{image}}^{3,2}\right) = 0 \end{aligned} \quad \text{(G.31)}$$

$$\begin{aligned} X_{1z} &= \mathbf{M}_{\mathbf{image}}^{1,3}\mathbf{M}_{\mathbf{image}}^{1,3} + C_1^2 + C_1^2\mathbf{M}_{\mathbf{image}}^{3,3}\mathbf{M}_{\mathbf{image}}^{3,3} + 2C_1\mathbf{M}_{\mathbf{image}}^{1,3}\mathbf{M}_{\mathbf{image}}^{3,3} \\ &= 2\tan^2(\theta_f)\cos^2(\phi_f) \\ X_{2z} &= 2\left(\mathbf{M}_{\mathbf{image}}^{1,3}\mathbf{M}_{\mathbf{image}}^{3,4} + z_pC_1 + z_pC_1\mathbf{M}_{\mathbf{image}}^{3,3}\mathbf{M}_{\mathbf{image}}^{3,3} + C_1\mathbf{M}_{\mathbf{image}}^{3,3}\mathbf{M}_{\mathbf{image}}^{3,4} + z_p\mathbf{M}_{\mathbf{image}}^{1,3}\mathbf{M}_{\mathbf{image}}^{3,3}\right) \\ &= 4z_p\tan(\theta_f)\cos(\phi_f) \end{aligned} \quad \text{(G.32)}$$

$$\begin{aligned} Y_{1x} &= \mathbf{M}_{\mathbf{image}}^{2,1}\mathbf{M}_{\mathbf{image}}^{2,1} + C_2^2\mathbf{M}_{\mathbf{image}}^{3,1}\mathbf{M}_{\mathbf{image}}^{3,1} + 2C_2\mathbf{M}_{\mathbf{image}}^{2,1}\mathbf{M}_{\mathbf{image}}^{3,1} = 0 \\ Y_{2x} &= 2x_f\left(\mathbf{M}_{\mathbf{image}}^{1,1}\mathbf{M}_{\mathbf{image}}^{2,1} + C_1C_2\mathbf{M}_{\mathbf{image}}^{3,1}\mathbf{M}_{\mathbf{image}}^{3,1} + C_1\mathbf{M}_{\mathbf{image}}^{2,1}\mathbf{M}_{\mathbf{image}}^{3,1} + C_2\mathbf{M}_{\mathbf{image}}^{1,1}\mathbf{M}_{\mathbf{image}}^{3,1}\right) \\ &\quad + 2\left(\mathbf{M}_{\mathbf{image}}^{2,1}\mathbf{M}_{\mathbf{image}}^{1,4} + z_pC_2\mathbf{M}_{\mathbf{image}}^{3,1}\mathbf{M}_{\mathbf{image}}^{3,1} + C_2\mathbf{M}_{\mathbf{image}}^{3,1}\mathbf{M}_{\mathbf{image}}^{1,4} + z_p\mathbf{M}_{\mathbf{image}}^{2,1}\mathbf{M}_{\mathbf{image}}^{3,1}\right) = 0 \end{aligned} \quad \text{(G.33)}$$

$$\begin{aligned} Y_{1y} &= 1 + \mathbf{M}_{\mathbf{image}}^{2,2}\mathbf{M}_{\mathbf{image}}^{2,2} + C_2^2\mathbf{M}_{\mathbf{image}}^{3,2}\mathbf{M}_{\mathbf{image}}^{3,2} + 2C_2\mathbf{M}_{\mathbf{image}}^{2,2}\mathbf{M}_{\mathbf{image}}^{3,2} = 2 \\ Y_{2y} &= 2x_f\left(\mathbf{M}_{\mathbf{image}}^{1,2}\mathbf{M}_{\mathbf{image}}^{2,2} + C_1C_2\mathbf{M}_{\mathbf{image}}^{3,2}\mathbf{M}_{\mathbf{image}}^{3,2} + C_1\mathbf{M}_{\mathbf{image}}^{2,2}\mathbf{M}_{\mathbf{image}}^{3,2} + C_2\mathbf{M}_{\mathbf{image}}^{1,2}\mathbf{M}_{\mathbf{image}}^{3,2}\right) \\ &\quad + 2\left(\mathbf{M}_{\mathbf{image}}^{2,2}\mathbf{M}_{\mathbf{image}}^{2,4} + z_pC_2\mathbf{M}_{\mathbf{image}}^{3,2}\mathbf{M}_{\mathbf{image}}^{3,2} + C_2\mathbf{M}_{\mathbf{image}}^{3,2}\mathbf{M}_{\mathbf{image}}^{2,4} + z_p\mathbf{M}_{\mathbf{image}}^{2,2}\mathbf{M}_{\mathbf{image}}^{3,2}\right) = 0 \end{aligned} \quad \text{(G.34)}$$

$$
\begin{aligned}
Y_{1z} &= \mathbf{M}_{\mathbf{image}}^{2,3}\mathbf{M}_{\mathbf{image}}^{2,3} + C_2^2 + C_2^2\mathbf{M}_{\mathbf{image}}^{3,3}\mathbf{M}_{\mathbf{image}}^{3,3} + 2C_2\mathbf{M}_{\mathbf{image}}^{2,3}\mathbf{M}_{\mathbf{image}}^{3,3} \\
&= 2\tan^2\left(\theta_f\right)\sin^2\left(\phi_f\right) \\
Y_{2z} &= 2x_f\left(\mathbf{M}_{\mathbf{image}}^{1,3}\mathbf{M}_{\mathbf{image}}^{2,3} + C_1C_2 + C_1C_2\mathbf{M}_{\mathbf{image}}^{3,3}\mathbf{M}_{\mathbf{image}}^{3,3} + C_1\mathbf{M}_{\mathbf{image}}^{2,3}\mathbf{M}_{\mathbf{image}}^{3,3} + C_2\mathbf{M}_{\mathbf{image}}^{1,3}\mathbf{M}_{\mathbf{image}}^{3,3}\right) \\
&\quad + 2\left(\mathbf{M}_{\mathbf{image}}^{2,3}\mathbf{M}_{\mathbf{image}}^{3,4} + z_pC_2 + z_pC_2\mathbf{M}_{\mathbf{image}}^{3,3}\mathbf{M}_{\mathbf{image}}^{3,3} + C_2\mathbf{M}_{\mathbf{image}}^{3,3}\mathbf{M}_{\mathbf{image}}^{3,4} + z_p\mathbf{M}_{\mathbf{image}}^{2,3}\mathbf{M}_{\mathbf{image}}^{3,3}\right) \\
&= 4x_f\tan^2\left(\theta_f\right)\sin\left(\phi_f\right)\cos\left(\phi_f\right) + 4z_p\tan\left(\theta_f\right)\sin\left(\phi_f\right)
\end{aligned}
\tag{G.35}
$$

$$
\begin{aligned}
C_x &= \mathbf{M}_{\mathbf{image}}^{1,4}\mathbf{M}_{\mathbf{image}}^{1,4} + z_p^2\mathbf{M}_{\mathbf{image}}^{3,1}\mathbf{M}_{\mathbf{image}}^{3,1} + 2z_p\mathbf{M}_{\mathbf{image}}^{3,1}\mathbf{M}_{\mathbf{image}}^{1,4} = 0 \\
C_y &= \mathbf{M}_{\mathbf{image}}^{2,4}\mathbf{M}_{\mathbf{image}}^{2,4} + z_p^2\mathbf{M}_{\mathbf{image}}^{3,2}\mathbf{M}_{\mathbf{image}}^{3,2} + 2z_p\mathbf{M}_{\mathbf{image}}^{3,2}\mathbf{M}_{\mathbf{image}}^{2,4} = 0 \\
C_z &= \mathbf{M}_{\mathbf{image}}^{3,4}\mathbf{M}_{\mathbf{image}}^{3,4} + z_p^2 + z_p^2\mathbf{M}_{\mathbf{image}}^{3,3}\mathbf{M}_{\mathbf{image}}^{3,3} + 2z_p\mathbf{M}_{\mathbf{image}}^{3,3}\mathbf{M}_{\mathbf{image}}^{3,4} = 2z_p^2.
\end{aligned}
\tag{G.36}
$$

In order to finish solving for the reflected voltage, Equation (G.28) is integrated along x_f and y_f. Integrating along y_f first yields

$$
\int_{-\infty}^{\infty} dy_f \exp\begin{pmatrix} -y_f^2\left(\frac{Y_{1x}}{w_x^2} + \frac{Y_{1y}}{w_y^2} + \frac{Y_{1z}}{w_z^2}\right) \\ -y_f\left(\frac{Y_{2x}}{w_x^2} + \frac{Y_{2y}}{w_y^2} + \frac{Y_{2z}}{w_z^2} + i\tilde{k}Y_k\right) \end{pmatrix} = \frac{\sqrt{\pi}}{\sqrt{\left(\frac{Y_{1x}}{w_x^2} + \frac{Y_{1y}}{w_y^2} + \frac{Y_{1z}}{w_z^2}\right)}} \exp\left(\frac{\left(\frac{Y_{2x}}{w_x^2} + \frac{Y_{2y}}{w_y^2} + \frac{Y_{2z}}{w_z^2} + i\tilde{k}Y_k\right)^2}{4\left(\frac{Y_{1x}}{w_x^2} + \frac{Y_{1y}}{w_y^2} + \frac{Y_{1z}}{w_z^2}\right)}\right)
$$

$$
= \frac{\sqrt{\pi}}{\sqrt{\left(\frac{2}{w_y^2} + \frac{2\tan^2\left(\theta_f\right)\sin^2\left(\phi_f\right)}{w_z^2}\right)}} \exp\left(\left(x_fY_{2z}' + Y_{2z}'' + i\tilde{k}Y_k'\right)^2\right)
$$

$$
= \frac{\sqrt{\pi}}{\sqrt{\left(\frac{2}{w_y^2} + \frac{2\tan^2\left(\theta_f\right)\sin^2\left(\phi_f\right)}{w_z^2}\right)}} \exp\begin{pmatrix} x_f^2\left(Y_{2z}'\right)^2 + 2x_f\left(Y_{2z}'Y_{2z}'' + i\tilde{k}Y_{2z}'Y_k'\right) \\ +\left(Y_{2z}''\right)^2 + 2i\tilde{k}Y_{2z}''Y_k' - \tilde{k}^2\left(Y_k'\right)^2 \end{pmatrix}, \tag{G.37}
$$

where

$$
Y_{2z}' = \frac{2\tan^2\left(\theta_f\right)\sin\left(\phi_f\right)\cos\left(\phi_f\right)}{w_z^2\sqrt{\left(\frac{2}{w_y^2} + \frac{2\tan^2\left(\theta_f\right)\sin^2\left(\phi_f\right)}{w_z^2}\right)}}
$$

$$
Y_{2z}'' = \frac{2z_p\tan\left(\theta_f\right)\sin\left(\phi_f\right)}{w_z^2\sqrt{\left(\frac{2}{w_y^2} + \frac{2\tan^2\left(\theta_f\right)\sin^2\left(\phi_f\right)}{w_z^2}\right)}} \tag{G.38}
$$

$$Y_k' = \frac{\tan\left(\theta_f\right)\sin\left(\phi_f\right)}{\sqrt{\left(\frac{2}{w_y^2} + \frac{2\tan^2\left(\theta_f\right)\sin^2\left(\phi_f\right)}{w_z^2}\right)}}.$$

Substituting the results from the integration back into Equation (G.28) then yields

$$V_{plane}(\omega) \cong \Omega(\omega)\frac{\sqrt{\pi}\exp\left(\left(Y_{2z}''\right)^2 + 2i\tilde{k}Y_{2z}''Y_k' - \tilde{k}^2\left(Y_k'\right)^2\right)}{\sqrt{\left(\frac{2}{w_y^2} + \frac{2\tan^2\left(\theta_f\right)\sin^2\left(\phi_f\right)}{w_z^2}\right)}}\exp\left(-\frac{2z_p^2}{w_z^2} - 2i\tilde{k}z_p\right)$$
$$\cdot\int_{-\infty}^{\infty} dx_f \left(\exp\left(\begin{array}{l} -x_f^2\left(\frac{X_{1x}}{w_x^2} + \frac{X_{1y}}{w_y^2} + \frac{X_{1z}}{w_z^2} - \left(Y_{2z}'\right)^2\right) \\ -x_f\left(\frac{X_{2x}}{w_x^2} + \frac{X_{2y}}{w_y^2} + \frac{X_{2z}}{w_z^2} + i\tilde{k}X_k\right) \\ -2\left(Y_{2z}'Y_{2z}'' + i\tilde{k}Y_{2z}'Y_k'\right)\end{array}\right)\right) \tag{G.39}$$

which can now be integrated along x_f. The integral along x_f is given by

$$\int_{-\infty}^{\infty} dx_f \left(\exp\left(\begin{array}{l} -x_f^2\left(\frac{X_{1x}}{w_x^2} + \frac{X_{1y}}{w_y^2} + \frac{X_{1z}}{w_z^2} - \left(Y_{2z}'\right)^2\right) \\ -x_f\left(\frac{X_{2x}}{w_x^2} + \frac{X_{2y}}{w_y^2} + \frac{X_{2z}}{w_z^2} + i\tilde{k}X_k\right) \\ -2\left(Y_{2z}'Y_{2z}'' + i\tilde{k}Y_{2z}'Y_k'\right)\end{array}\right)\right) = \frac{\sqrt{\pi}}{\sqrt{\left(\frac{X_{1x}}{w_x^2} + \frac{X_{1y}}{w_y^2} + \frac{X_{1z}}{w_z^2} - \left(Y_{2z}'\right)^2\right)}}$$
$$\cdot\exp\left(\frac{\left(\begin{array}{l}\left(\frac{X_{2x}}{w_x^2} + \frac{X_{2y}}{w_y^2} + \frac{X_{2z}}{w_z^2} + i\tilde{k}X_k\right)^2 \\ -2\left(Y_{2z}'Y_{2z}'' + i\tilde{k}Y_{2z}'Y_k'\right)\end{array}\right)}{4\left(\frac{X_{1x}}{w_x^2} + \frac{X_{1y}}{w_y^2} + \frac{X_{1z}}{w_z^2} - \left(Y_{2z}'\right)^2\right)}\right)$$

$$= \frac{\sqrt{\pi}\exp\left(\dfrac{\left(\dfrac{2z_p\tan\left(\theta_f\right)\cos\left(\phi_f\right)}{w_z^2}+i\widetilde{k}\tan\left(\theta_f\right)\cos\left(\phi_f\right)-\left(Y_{2z}'Y_{2z}''+i\widetilde{k}Y_{2z}'Y_k'\right)\right)^2}{\left(\dfrac{2}{w_x^2}+\dfrac{2\tan^2\left(\theta_f\right)\cos^2\left(\phi_f\right)}{w_z^2}-\left(Y_{2z}'\right)^2\right)}\right)}{\sqrt{\left(\dfrac{2}{w_x^2}+\dfrac{2\tan^2\left(\theta_f\right)\cos^2\left(\phi_f\right)}{w_z^2}-\left(Y_{2z}'\right)^2\right)}}. \quad \text{(G.40)}$$

As a result, the voltage returned from the plane is given by

$$V_{plane}(\omega) \cong \frac{\pi\Omega(\omega)\exp\left(\left(Y_{2z}''\right)^2+2i\widetilde{k}Y_{2z}''Y_k'-\widetilde{k}^2\left(Y_k'\right)^2\right)\exp\left(-\dfrac{2z_p^2}{w_z^2}-2i\widetilde{k}z_p\right)}{\sqrt{\left(\dfrac{2}{w_y^2}+\dfrac{2\tan^2\left(\theta_f\right)\sin^2\left(\phi_f\right)}{w_z^2}\right)\left(\dfrac{2}{w_x^2}+\dfrac{2\tan^2\left(\theta_f\right)\cos^2\left(\phi_f\right)}{w_z^2}-\left(Y_{2z}'\right)^2\right)}}$$
$$\cdot\exp\left(\frac{\left(\dfrac{2z_p\tan\left(\theta_f\right)\cos\left(\phi_f\right)}{w_z^2}+i\widetilde{k}\tan\left(\theta_f\right)\cos\left(\phi_f\right)-\left(Y_{2z}'Y_{2z}''+i\widetilde{k}Y_{2z}'Y_k'\right)\right)^2}{\left(\dfrac{2}{w_x^2}+\dfrac{2\tan^2\left(\theta_f\right)\cos^2\left(\phi_f\right)}{w_z^2}-\left(Y_{2z}'\right)^2\right)}\right). \quad \text{(G.41)}$$

Equation (G.41) can be simplified further by assuming that θ_f is small, allowing all terms to the fourth power of $\sin\left(\theta_f\right)$ to be ignored. Hence

$$\left(Y_{2z}'\right)^2 = \frac{4\tan^4\left(\theta_f\right)\sin^2\left(\phi_f\right)\cos^2\left(\phi_f\right)}{w_z^4\left(\dfrac{2}{w_y^2}+\dfrac{2\tan^2\left(\theta_f\right)\sin^2\left(\phi_f\right)}{w_z^2}\right)} \cong 0 \quad \text{(G.42)}$$

$$\left(Y_{2z}''\right)^2+2i\widetilde{k}Y_{2z}''Y_k'-\widetilde{k}^2\left(Y_k'\right)^2 = \frac{\tan^2\left(\theta_f\right)\sin^2\left(\phi_f\right)}{\left(\dfrac{2}{w_y^2}+\dfrac{2\tan^2\left(\theta_f\right)\sin^2\left(\phi_f\right)}{w_z^2}\right)}\left(\frac{4z_p^2}{w_z^4}+i\widetilde{k}\frac{4z_p}{w_z^2}-\widetilde{k}^2\right) \quad \text{(G.43)}$$
$$\cong \frac{w_y^2\tan^2\left(\theta_f\right)\sin^2\left(\phi_f\right)}{2}\left(\frac{4z_p^2}{w_z^4}+i\widetilde{k}\frac{4z_p}{w_z^2}-\widetilde{k}^2\right)$$

$$\left(Y'_{2z}Y''_{2z}+i\tilde{k}Y'_{2z}Y'_{k}\right)=\frac{4z_p\tan^3\left(\theta_f\right)\sin^2\left(\phi_f\right)\cos\left(\phi_f\right)}{w_z^4\left(\frac{2}{w_y^2}+\frac{2\tan^2\left(\theta_f\right)\sin^2\left(\phi_f\right)}{w_z^2}\right)}+i\tilde{k}\frac{2\tan^3\left(\theta_f\right)\sin^2\left(\phi_f\right)\cos\left(\phi_f\right)}{w_z^2\left(\frac{2}{w_y^2}+\frac{2\tan^2\left(\theta_f\right)\sin^2\left(\phi_f\right)}{w_z^2}\right)}$$

$$=\frac{\tan^3\left(\theta_f\right)\sin^2\left(\phi_f\right)\cos\left(\phi_f\right)}{w_z^2\left(\frac{1}{w_y^2}+\frac{\tan^2\left(\theta_f\right)\sin^2\left(\phi_f\right)}{w_z^2}\right)}\left(\frac{2z_p}{w_z^2}+i\tilde{k}\right) \tag{G.44}$$

$$\cong\frac{w_y^2\tan^3\left(\theta_f\right)\sin^2\left(\phi_f\right)\cos\left(\phi_f\right)}{w_z^2}\left(\frac{2z_p}{w_z^2}+i\tilde{k}\right).$$

Substituting Equations (G.42), (G.43), and (G.44) into Equation (G.41) then yields

$$V_{plane}(\omega)\cong\frac{\pi\Omega(\omega)\exp\left(\frac{w_y^2\tan^2\left(\theta_f\right)\sin^2\left(\phi_f\right)}{2}\left(\frac{4z_p^2}{w_z^4}+i\tilde{k}\frac{4z_p}{w_z^2}-\tilde{k}^2\right)\right)\exp\left(-\frac{2z_p^2}{w_z^2}-2i\tilde{k}z_p\right)}{\sqrt{\left(\frac{2}{w_y^2}+\frac{2\tan^2\left(\theta_f\right)\sin^2\left(\phi_f\right)}{w_z^2}\right)\left(\frac{2}{w_x^2}+\frac{2\tan^2\left(\theta_f\right)\cos^2\left(\phi_f\right)}{w_z^2}\right)}}$$

$$\cdot\exp\left(\frac{\tan^2\left(\theta_f\right)\cos^2\left(\phi_f\right)\left(\frac{4z_p^2}{w_z^4}+i\tilde{k}\frac{4z_p}{w_z^2}-\tilde{k}^2\right)\left(1-\frac{w_y^2\tan^2\left(\theta_f\right)\sin^2\left(\phi_f\right)}{w_z^2}\right)^2}{\left(\frac{2}{w_x^2}+\frac{2\tan^2\left(\theta_f\right)\cos^2\left(\phi_f\right)}{w_z^2}\right)}\right)$$

$$\cong\frac{\pi w_x w_y\Omega(\omega)\exp\left(\frac{w_y^2\tan^2\left(\theta_f\right)\sin^2\left(\phi_f\right)}{2}\left(\frac{4z_p^2}{w_z^4}+i\tilde{k}\frac{4z_p}{w_z^2}-\tilde{k}^2\right)\right)\exp\left(-\frac{2z_p^2}{w_z^2}-2i\tilde{k}z_p\right)}{2\sqrt{1+\frac{w_x^2\tan^2\left(\theta_f\right)\cos^2\left(\phi_f\right)}{w_z^2}+\frac{w_y^2\tan^2\left(\theta_f\right)\sin^2\left(\phi_f\right)}{w_z^2}}}$$

$$\cdot\exp\left(\frac{w_x^2\tan^2\left(\theta_f\right)\cos^2\left(\phi_f\right)}{2}\left(\frac{4z_p^2}{w_z^4}+i\tilde{k}\frac{4z_p}{w_z^2}-\tilde{k}^2\right)\right)$$

$$\cong \frac{\pi w_x w_y \Omega(\omega) \exp\left(-\frac{2z_p^2}{w_z^2} - 2i\tilde{k}z_p\right)}{2}\left(1 - \frac{w_x^2 \tan^2(\theta_f)\cos^2(\phi_f)}{2w_z^2} - \frac{w_y^2 \tan^2(\theta_f)\sin^2(\phi_f)}{2w_z^2}\right)$$
$$\cdot \exp\left(\frac{w_y^2 \tan^2(\theta_f)\sin^2(\phi_f)}{2}\left(\frac{4z_p^2}{w_z^4} + i\tilde{k}\frac{4z_p}{w_z^2} - \tilde{k}^2\right)\right)$$
$$\cdot \exp\left(\frac{w_x^2 \tan^2(\theta_f)\cos^2(\phi_f)}{2}\left(\frac{4z_p^2}{w_z^4} + i\tilde{k}\frac{4z_p}{w_z^2} - \tilde{k}^2\right)\right). \tag{G.45}$$

The value for $\Omega(\omega)$ can now be substituted in from Equation (G.20) to get the complete expression for the voltage returned from an inclined plane placed near the focus, that is,

$$\begin{aligned} V_{plane}(\omega) \cong & \frac{-w_x w_y \tilde{k}^2 \Gamma_{plane} V_{inc}(\omega) H^2(\omega) G_o^2 \cos(\theta_f)}{8\pi S_T} e^{i2\tilde{k}z_T} e^{-\frac{2z_p^2}{w_z^2}} \\ & \cdot \left(1 - \frac{\tan^2(\theta_f)}{2w_z^2}\left(w_x^2 \cos^2(\phi_f) + w_y^2 \sin^2(\phi_f)\right)\right) \\ & \cdot \exp\left(-i2\tilde{k}z_p\left(1 - \frac{\tan^2(\theta_f)}{w_z^2}\left(w_x^2 \cos^2(\phi_f) + w_y^2 \sin^2(\phi_f)\right)\right)\right) \\ & \cdot \exp\left(-\tilde{k}^2 \frac{\tan^2(\theta_f)}{2}\left(w_x^2 \cos^2(\phi_f) + w_y^2 \sin^2(\phi_f)\right)\right), \end{aligned} \tag{G.46}$$

where it is assumed that $4z_p^2 / w_z^4 << \tilde{k}^2$. Also, because $w_x, w_y << w_z$, Equation (G.46) can be further simplified to yield

$$\begin{aligned} V_{plane}(\omega) \cong & \frac{-w_x w_y \tilde{k}^2 \Gamma_{plane} V_{inc}(\omega) H^2(\omega) G_o^2 \cos(\theta_f)}{8\pi S_T} e^{i2\tilde{k}(z_T - z_p)} e^{-\frac{2z_p^2}{w_z^2}} \\ & \cdot \exp\left(-\tilde{k}^2 \frac{\tan^2(\theta_f)}{2}\left(w_x^2 \cos^2(\phi_f) + w_y^2 \sin^2(\phi_f)\right)\right). \end{aligned} \tag{G.47}$$

Now that an expression for the voltage returned from the inclined plane has been derived, the equation can be checked by considering a special case. First, if $w_x = w_y$, as would be the case for circularly symmetric source, Equation (G.47) becomes

$$V_{plane}(\omega) \cong \frac{-w_x^2 \tilde{k}^2 \Gamma_{plane} V_{inc}(\omega) H^2(\omega) G_o^2 \cos(\theta_f)}{8\pi S_T} e^{i2\tilde{k}(z_T - z_p)} e^{-\frac{2z_p^2}{w_z^2} - w_x^2 \tilde{k}^2 \frac{\tan^2(\theta_f)}{2}}, \qquad \text{(G.48)}$$

which is no longer dependent on the angle ϕ_f as would be expected. Secondly, if θ_f goes to zero, Equation (G.47) becomes

$$V_{plane}(\omega) \cong \frac{-w_x w_y \tilde{k}^2 \Gamma_{plane} V_{inc}(\omega) H^2(\omega) G_o^2}{8\pi S_T} e^{i2\tilde{k}(z_T - z_p)} e^{-\frac{2z_p^2}{w_z^2}}, \qquad \text{(G.49)}$$

which is the same as was derived previously for a plane placed parallel to the focal plane in Chapter 2.

In order to validate Equation (G.48), experiments were performed using a piece of smooth Plexiglas to act as the rigid plane placed near the focal plane of a spherically focused *f*/2 transducer (Valpey Fisher Instruments, Inc., Hopkinton, MA). The transducer had a diameter of 2.1 cm, a center frequency of 8.7 MHz, and a –3 dB bandwidth of 1.6 MHz as measured from a wire reflection [*Raum and O'Brien*, 1997]. Also, the equivalent Gaussian dimensions for the transducer were measured in Chapter 3 and were found to be $w_z = 17.1\lambda + 924 \cdot 10^{-6}$ m and $w_x = 1.57\lambda + 27.0 \cdot 10^{-6}$ m. The transducer was placed in a water bath and shock excited using a Panametrics 5900 pulser/receiver (Waltham, MA) operating in pulse-echo mode, and the returned waveforms were recorded using a digital oscilloscope at a sampling frequency of 100 MHz (Lecroy 9354 TM; Chestnut Ridge, NY) and averaged 100 times. The Plexiglas plate was placed at focal plane by positioning the plate so that the pulse-echo peak-to-peak voltage was a maximum. The Plexiglas was then rotated so that θ_f swept out angles from -10^o to 10^o, while maintaining a z_o of approximately zero, and the pulse echo waveform was recorded for every 1^o change of θ_f. The scan was repeated four times with focus moved along the axis of rotation for the plate in steps of 0.1 mm (i.e. 0 mm, 0.1 mm, 0.2 mm, and 0.3 mm). The results at each angle for all four scans were then averaged together. Also, the value of z_p was then estimated from the location of the time-domain waveforms and the corresponding spectra were multiplied by $\exp\left(2\left(z_p / w_z\right)^2\right)$. However, the correction term for z_p did not significantly effect the final results (max value for $|z_p|$ of 395 μm).

A comparison between the measured backscattered waveforms $V_{measured}$ and the derived theory V_{theory} is given in Figure G.2 where the curve was calculated from

$$ASD_{plane}\left(\theta_f\right) = 10 \cdot \log_{10}\left(\underset{\forall \omega}{\text{mean}}\left(\left(\frac{V_{measured}(\omega) - V_{theory}(\omega)}{\underset{\forall \omega}{\max}\left(V_{measured}(\omega)\big|_{\theta_f = 0} \right)} \right)^2 \right) \right), \tag{G.50}$$

where

$$V_{theory}(\omega) = \left(V_{measured}(\omega)\big|_{\theta_f = 0} \right) \cos\left(\theta_f\right) e^{-w_x^2 \tilde{k}^2 \frac{\tan^2\left(\theta_f\right)}{2}}. \tag{G.51}$$

Clearly there is very good agreement between the theoretical and experimental results for all of the inclination angles of the plane.

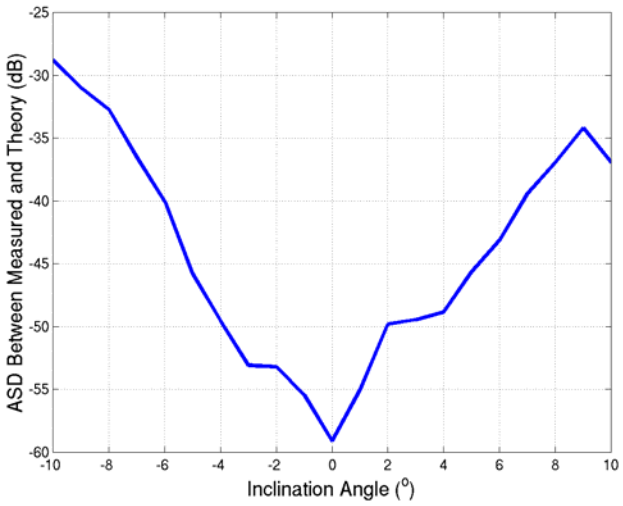

Figure G.2: A comparison between the measured backscattered waveforms and the derived theory for various inclination angles of plane placed at the focus.

Recall that the purpose of the derivation was to use the inclined plane to approximate the skull interface of the developing fetus. The backscattered signals from the developing skull could then be analyzed to assess properties such as attenuation of the intervening tissue layers. Hence, the experimental results were also evaluated in terms of the accuracy of the attenuation estimate that would have resulted from the backscattered signals at each inclination angle of the plane. Because the inclination angle of the skull relative to the incident ultrasound beam would not be known *in vivo* (at least for a traditional 2D imaging system), the estimate of the attenuation assumed that w_x was strictly proportional to the wavelength (i.e., assumed diffraction limited). Hence, $V_{plane}(\omega)$ would have the same exact shape for all incident angles. One traditional method for calculating the attenuation is to monitor the down shift in the peak frequency relative to the assumed Gaussian bandwidth for the source [*Narayana and Ophir*,

1983]. Using this theory, the error in the attenuation estimate for different inclination angles would be given by

$$\alpha_{error} = \frac{f_{peak}\left(\theta_f = 0\right) - f_{peak}\left(\theta_f\right)}{2\sigma_{\omega p}^2}, \tag{G.52}$$

where f_{peak} is the frequency corresponding to the spectral peak at each inclination angle, and the spectrum of the signal returned from the plane is approximately proportional to $\exp\left(-\left(\frac{f - f_{peak}}{2\sigma_{\omega p}^2}\right)^2\right)$.

Figure G.3a shows the error in the attenuation after fitting a Gaussian to the backscattered voltage spectrum from the plate at various inclination angles calculated using Equation (G.52). The frequencies selected for the fit were all the frequencies for which the backscattered voltage spectrum was greater than ½ its peak value for a θ_f of 0^o (7.29 MHz to 9.79 MHz). The magnitude of the voltage at the spectral peak for each value of θ_f relative to the value for a θ_f of zero degrees is also provided (Figure G.3b). The error introduced by θ_f is small (less than 0.1 dB/MHz) for angles from -6^o to greater than 10^o. Also, the magnitude of the backscatter decreases quickly with increasing inclination angle of the Plexiglas plate. Hence, the most reliable attenuation estimates would be obtained when the ultrasound beam was impinging on the specular scatterer close to normal incidence.

After completing the experiments using a Plexiglas plate, the external surface of the skull plate of an adult rat was exposed using the same experimental system. The skull was obtained from a rat that had been euthanized in a humane fashion as part of another experiment. First, the skin on the head was trimmed away. Then, the top portion of the skull was cut using scissors from the eyes to the ears. The cut skull was then pulled gently from the brain and the connective tissue was trimmed away from both sides of the removed skull plate. Finally, the skull was rinsed and placed in a sterile saline solution. The skull/saline solution was refrigerated for several days before the ultrasound experiment was performed.

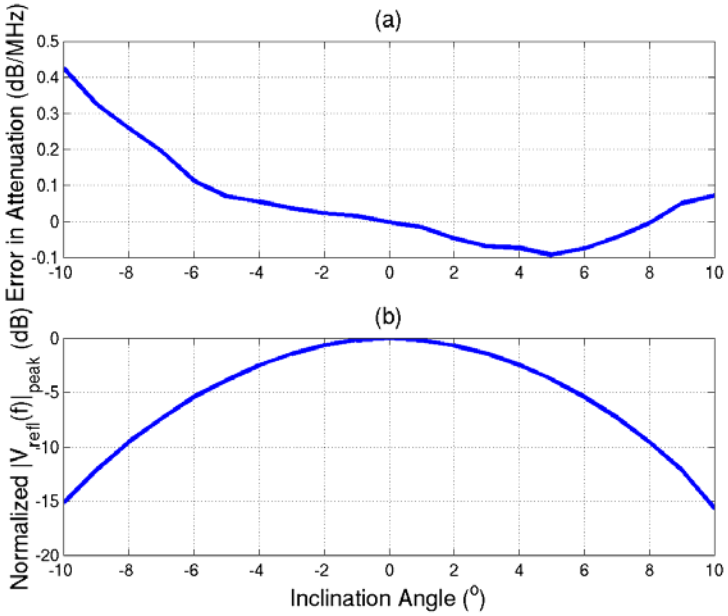

Figure G.3: (a) Error in attenuation estimates resulting from inclination angle, and (b) normalized magnitude of spectrum peak of backscattered signal for various inclination angles of the Plexiglas plate.

Once again, the skull was positioned so that the focus would be on the outer surface of the skull with the beam at approximately normal incidence by adjusting the position of the skull and transducer to achieve the maximum peak-to-peak voltage of the backscattered time domain waveform. The skull was then rotated so that the inclination angle of the beam would change from -10^o to $+10^o$ and the backscattered waveform from the skull was recorded every 1^o. However, the axis of rotation did not coincide with the focus so the value of z_p changed as the skull was rotated (max value for $|z_p|$ of 1.15 mm). After acquiring the waveforms the impact of z_p was once again removed by analyzing the time-domain signals, and the error in the attenuation for each value of inclination angle was found from Equation (G.52). The error in attenuation and the magnitude of the voltage at the spectral peak for each inclination angle relative to the magnitude of the voltage at the spectral peak for the Plexiglas for a θ_f of zero degrees are shown in Figure G.4. The magnitude signal from the skull (Figure G.4b) is much less than the magnitude of the signal from the Plexiglas plate. Also, the magnitude does not decay as quickly with increasing inclination angle. This probably results from roughness on the surface of the skull introducing diffuse scattering. Also, the error in the attenuation estimate is small over the entire range of inclination angles. This may also result from the diffuse scatterers reducing the impact of the incident angle, but further experiments are required before this hypothesis can be

validated. Regardless, the results in Figure G.4 demonstrate the potential for obtaining an estimate of the attenuation along the propagation path in *in vivo* exposures of the developing human skull.

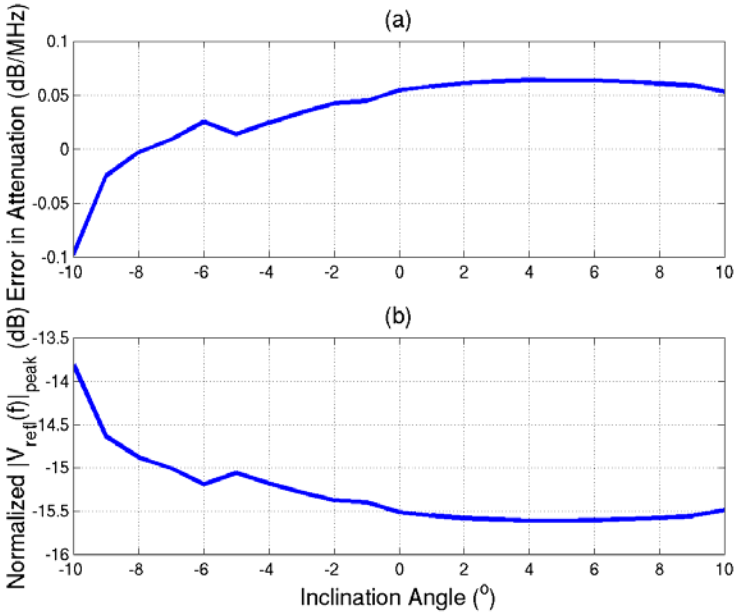

Figure G.4: (a) Error in attenuation estimates resulting from inclination angle, and (b) normalized magnitude of spectrum peak of backscattered signal for various inclination angles of the rat skull.